Nanostructure Growth on Rhodium/Ruthenium by the Exposure to He Plasma*)

Tomohiro NOJIMA, Shin KAJITA[1)], Naoaki YOSHIDA[2)], Shota KAWAGUCHI, Noriyasu OHNO, Hirohiko TANAKA, Masayuki TOKITANI[3)], Daisuke NAGATA[3)], Tsuyoshi AKIYAMA[3)] and Takashi YAGI[4)]

Graduate School of Engineering, Nagoya University, Nagoya 464-8603, Japan
[1)]*Institute of Materials and Systems for Sustainability, Nagoya University, Nagoya 464-8603, Japan*
[2)]*Research Institute for Applied Mechanics, Kyushu University, Fukuoka 819-0395, Japan*
[3)]*National Institute for Fusion Science, Toki 509-5292, Japan*
[4)]*National Institute of Advanced Industrial Science and Technology, Tsukuba 305-8563, Japan*

(Received 28 December 2017 / Accepted 18 April 2018)

Rhodium and ruthenium thin film coatings were conducted on tungsten samples by using a magnetron sputtering device; then, we irradiated He plasma to the samples in the linear plasma device NAGDIS-II (Nagoya Divertor Simulator). Fuzzy nanostructures were formed on rhodium and ruthenium samples when the surface temperatures were ~950 and ~1200 K, respectively. When the surface temperature was high, i.e., >1200 K, it was found that tungsten atoms diffused across the rhodium film and reached the film surface, and tungsten-fuzz was formed over the rhodium layer. From TEM analysis of ruthenium fibers, it was identified that there were thin parts in the fibers, and some fibers had no He bubbles. It was likely that fiber growth mechanism on ruthenium was different from the other metals.

Keywords: rhodium, ruthenium, fuzz, percolation, morphology change

DOI: 10.1585/pfr.13.3406065

1. Introduction

Fiber-form nanostructure (fuzz) growth is one of the key issues in plasma-wall interactions, because it may be formed on tungsten divertor under fusion relevant conditions [1]. It is concerned that fuzz formed on divertor wall induces the formation of impurities and deteriorates confinement performance in fusion reactors. On the other hand, fuzz is expected to be applied to enhance catalysis activity by increasing surface area [2].

In order to advance studies concerning fuzz, it is necessary to make the formation mechanism clear. Although some formation models have been suggested [3–5], the fuzz growth mechanism has yet to be explained well, as well as nano tendril bundle (NTB) [6] and large scale nanostructures [7].

The viscoelastic model proposed by S. Krasheninnikov suggested that shear stress induced by embedded He atoms could be a driving force of tungsten (W) fuzz growth [3]. And a molecular dynamics (MD) simulation showed that yield strength of W fiber reduces significantly when He atoms were embedded [8]. Following these studies, the relationship between fuzz formation and shear modulus was discussed [9]; the fuzz was easily formed on high shear modulus metals such as W, Molybdenum (Mo) and rhenium (Re), [10–12]. However, morphology changes induced by He plasma irradiation were not well-researched in other high shear modulus metals including rhodium (Rh) and ruthenium (Ru), which are face-centered cubic (FCC) and hexagonal close-packed (HCP), respectively. The shear modulus of Rh and Ru is 152 and 173 GPa at room temperature (R.T) [13, 14], respectively, which are comparable or higher than that of W (160 GPa at R.T).

In this study, we show the morphology changes of Rh and Ru surfaces by the He plasma irradiation and discuss the mechanism of fuzz formation.

2. Experimental Setup

Rh and Ru thin film coatings were conducted on W samples using a magnetron sputtering device. The thickness of Rh and Ru was approximately 1 and 2 μm, respectively. The He plasma irradiations were conducted in the linear plasma device NAGDIS-II (Nagoya Divertor Simulator) [15]. High density plasmas, typically 10^{18} - 10^{19} m^{-3}, can be produced in steady state. The incident ion energy was controlled by changing the biasing of the samples, and the sample temperature was measured by a radiation pyrometer. The emissivity of Rh and Ru at 1.6 μm was assumed to be 0.18 and 0.20, respectively. When the samples were irradiated at temperature lower than 1000 K, they

author's e-mail: nojima-tomohiro@ees.nagoya-u.ac.jp
*) This article is based on the presentation at the 26th International Toki Conference (ITC26).

were mounted on a water cooling stage. When the surface temperature was higher than 1000 K, samples were spot-welded to an electrode. In those cases, the temperature was determined by the balance between the heat flux from the plasma and the radiation from the sample. After the He plasma irradiation, the samples were analyzed by scanning electron microscope (SEM), transmission electron microscope (TEM), energy dispersive X-ray spectrometry (EDS) and thermal desorption spectroscopy (TDS).

3. Results and Discussion

3.1 Ruthenium (Ru)

He plasma irradiation was conducted at the incident ion energy of 45 eV as changing the surface temperature from 1123 to 1523 K, as shown in Table 1. The He fluence was on the order of 10^{25} m^{-2}.

Figures 1 (a-c) show the SEM micrographs of Ru sample exposed to He plasmas when the surface temperatures were 1193, 1383 and 1523 K, respectively. Fuzz was formed on the Ru sample when the surface temperature was 1193 K. As shown in Fig. 1 (b), rough surface with fibers was observed when the surface temperature was 1373 K. It was likely that fuzz was difficult to be formed on Ru surface at this temperature. A large scale wavy surface was observed when the surface temperature was 1523 K.

Figures 2 (a-c) show the EDS and TEM analysis of Ru sample exposed to He plasma when the surface temperature was 1193 K. Figure 2 (a) shows distributions of Ru and W atoms with green and red colored maps, respectively. It was found that W atoms diffused to Ru layer during the plasma irradiation. The thickness of the Ru layer was originally 2 μm and W atoms diffused to the half bottom of the layer. On the top of the layer and the fibers, the ratio of the number of Ru atoms to that of W atoms was about 10. Therefore, it can be said that Ru comprised the fibers.

Figures 2 (b, c) show the TEM micrographs of fiber region. It was identified that Ru fibers grew linearly different from W fuzz [16]. On the other hand, He bubbles were observed in thick regions of fibers and node parts. The formation of He bubbles was commonly observed in fibers after He plasma irradiation [16]. Elliptical He bubbles were observed in Ru fibers, as shown in the inset of Fig. 2 (b) which have not been observed in W. On the other hand, no He bubbles were observed in narrow parts of Ru fibers.

Linear fiber growth was also observed on Re surface

Table 1 Summary of the condition of the irradiation experiments and results of Ru.

Temp. [K]	Energy [eV]	He Fluence $\times 10^{25}$[m^{-2}]	Morphology changes
1123	45	2.4	Fuzz
1193	45	3.3	Fuzz
1383	45	1.6	Rough surface with fibers
1523	45	3.0	Wavy structure

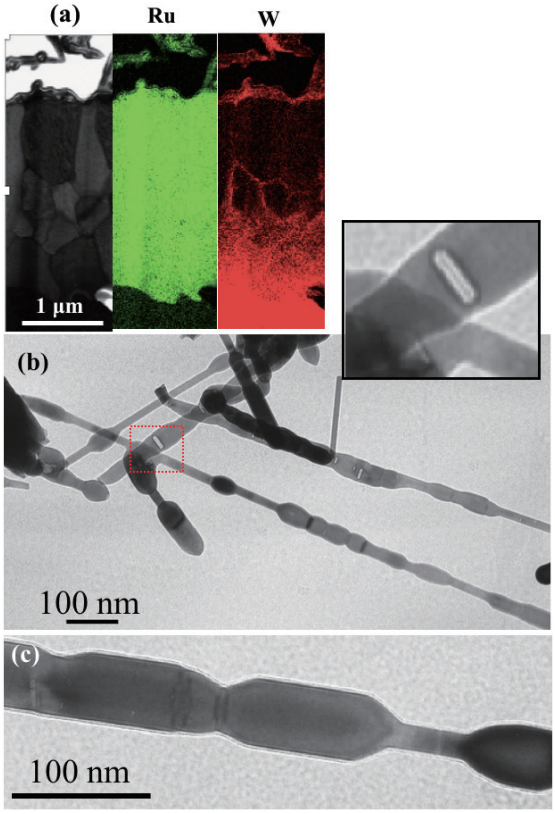

Fig. 2 (a) TEM micrographs and EDS mappings of Ru (green) and W (red), and (b, c) TEM micrographs of Ru sample exposed to He plasma at surface temperature was 1193 K.

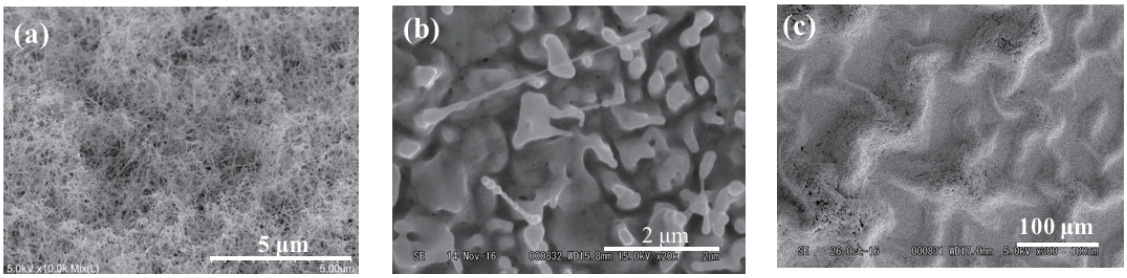

Fig. 1 SEM micrographs of Ru sample exposed to He plasmas at the surface temperature of (a) 1193, (b) 1373 and (c) 1523 K.

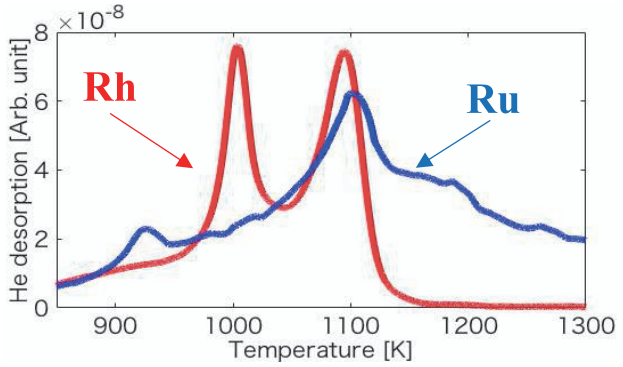

Fig. 3 TDS spectrums from Rh (red line) and Ru samples (blue line) exposed to the He plasmas. The irradiation conditions of Rh and Ru were the followings: surface temperature was 923 K and 1383 K, fluence was 1.6×10^{25} and 8.9×10^{25} m^{-2}, respectively. Incident ion energy was 45 eV. Heating rates of Ru and Rh samples were 0.26 and 0.17 K/s, respectively.

exposed to He plasma at high surface temperature [9]. It is noted that the crystal structure of Ru and Re is HCP. All the metals on which fuzz formation was confirmed have body centered cubic (BCC) or FCC other than Ru and Re, as was shown in [17]. In addition, although the relationship between fuzz formation and shear modulus was updated in [17], linear fiber growth was not identified on matals with BCC or FCC crystal structures. Thus, the results indicated that linear fiber growth was related to crystal structure; it is of interest to investigate the crystal orientation similar to the analysis recently reported on W [18].

A blue curve in Fig. 3 shows the TDS spectrum of He desorption from Ru samples exposed to He plasma. A He desorption peak was observed at 1100 K. On W, there were two TDS peaks around the lower and upper temperature limits for the fuzz growth [19]; the results suggested that He migration was deeply related with the morphology changes. Similarly, it was likely that He migration was activated around this temperature and fuzz was observed at 1123 - 1193 K. Although we conducted the TDS up to 1300 K, it is likely that another peak will appear above 1300 K considering the fact that the structure became greater probably due to significant He migration.

3.2 Rhodium (Rh)

Table 2 summarizes the irradiation condition for Rh irradiation experiments. The incident ion energy was fixed at 45 eV, and the surface temperature was changed from 613 to 1633 K; the fluence was higher than 10^{25} m^{-2}.

Significant surface morphology changes were not observed from SEM analysis when the surface temperature was 613 K. From TEM analysis, however, nano bubbles and dislocation loops were observed in the surface region, as shown in Fig. 4. Surface roughness seems to be induced by sputtering of incident He atoms. Recently, He plasma irradiation to Rh sample at 510 - 550 K was conducted by

Table 2 Summary of the condition of the irradiation experiments and results of Rh.

Temp. [K]	Energy [eV]	He Fluence $\times 10^{25}$[m^{-2}]	Morphology changes
613	45	1.4	No change
923	45	8.9	Fuzz
973	45	11	Fuzz
1203	45	2.1	Fiber and micro structure
1323	45	2.6	Micro structure
1473	45	3.4	Micro structure
1633	45	5.6	Micro structure

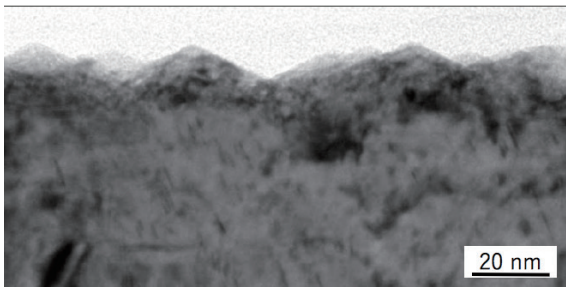

Fig. 4 TEM micrograph of Rh sample exposed to He plasma at the temperature of 613 K.

Litnovsky *et al.* [20], and slight reduction in the optical reflectance was identified. It was likely that reduction in the optical reflectance became greater as increasing the surface temperature because of an enhancement of roughness.

Figures 5 (a-c) present an SEM and TEM micrographs, and EDS mapping of Rh samples exposed to the He plasma at the surface temperature of 973 K, respectively. Fuzz was formed on Rh sample. The distributions of W and Rh atoms are shown as green and red images, respectively, in Fig. 5 (b). It is seen that fuzz formed at 973 K mainly consists of Rh and some W atoms diffused from the substrate to original Rh layer. The ratio of Rh atoms and W ones in the bottom part of Rh layer was 2 to 1; it is likely that an intermediate layer (ε-layer), different from BCC in W and FCC in Rh, was formed from Rh-W phase diagram [21]. On the other hand, the fraction of W in Rh fiber was negligible. From Fig. 5 (c), it is seen that elliptical He bubbles were observed in addition to round shaped He bubbles. The elliptical shaped bubbles in fibers were always axially suppressed and radially elongated. It is noted that elliptical shaped bubbles have not been identified in W cases.

In Fig. 3, TDS spectrum for Rh sample was also shown. The gas desorption was terminated around 1150 K. This indicated that He atoms were sufficiently desorbed from Rh sample at about 1150 K and that the fuzz growth only occurs when the surface temperature was below ~ 1100 K on Rh.

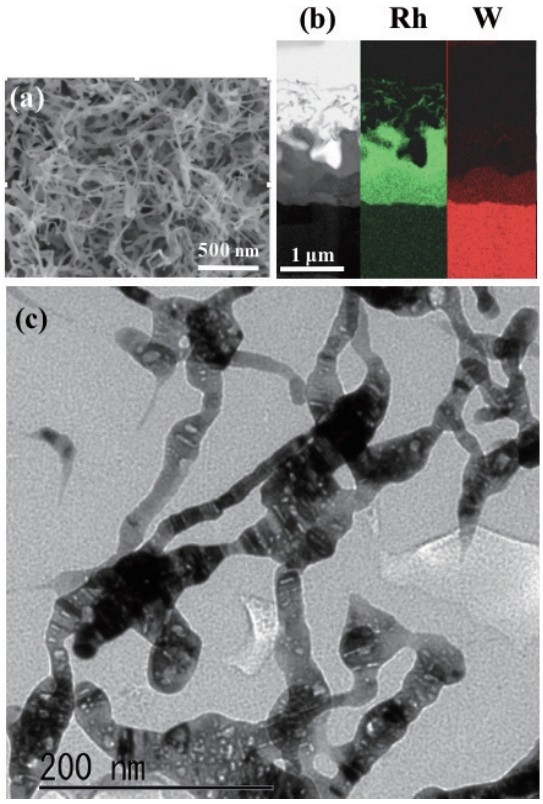

Fig. 5 (a) SEM, (b, c) TEM/EDS micrographs of Rh samples exposed to He plasma at the surface temperature of 973 K.

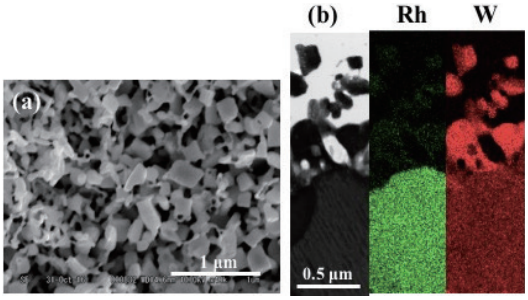

Fig. 6 (a) SEM and (b) TEM of Rh samples exposed to He plasma at the surface temperature of 1323 K.

SEM and TEM micrographs with EDS mappings for the sample exposed to the He plasma at a higher surface temperature of 1323 K were shown in Figs. 6 (a) and (b), respectively. Microstructure similar to the sample shown in Fig. 6 (a) was formed on the surface. From EDS analysis shown in Fig. 6 (b), it mainly consisted of W, not Rh atom, indicating that W atoms in the substrate actively diffused at 1323 K and percolated on the Rh layer, the thickness of which was about 1 μm. Percolation was also observed when the surface temperature was 1633 K, and the fluence was 5.6×10^{25} He/m^2. Percolation was observed when the surface temperature was higher than 1300 K. Probably an increase of the diffusion coefficient of W with increasing the temperature has led to this phenomenon.

4. Conclusion

He plasma irradiations were conducted using the linear plasma device NAGDIS-II to Rh and Ru films deposited on tungsten sample. Fiber-form nanostructure (fuzz) was formed on Ru and Rh when the surface temperate was in the range of 1100 - 1200 and 900 - 1000 K, respectively. In comparison with fuzz formation temperature of W, which was in the range of $0.27 < T_s/T_m$ (T_s; surface temperature, T_m; melting point) < 0.54 [10], the fuzz formation condition was within the same range, but was narrower (0.42 - 0.46 for Ru and 0.40 - 0.44 for Rh).

There were no significant morphology changes on Rh surface exposed to He plasma at the surface temperature of 613 K. Percolation of W atoms was observed on Rh samples when the surface temperature was higher than 1323 K or higher.

It was noted that both metals have high shear modulus. Because fuzzy structure was formed on both metals easily with the He fluence of the order of 10^{25} m^{-2}, the present results support the fact that fuzzy structure can be easily grown on high shear modulus metals. On Ru surface, linear fiber growth was observed. It was likely that crystal structure is related to linear fiber growth. On metals with HCP crystal structure, He plasma induced fibers could be grown linearly different from BCC or FCC metals.

Acknowledgments

This work was supported in part by a Grant-in-Aid for Scientific Research (B) 15H04229, a Grant-in-Aid for Exploratory Research 16K13917 from the Japan Society for the Promotion of Science (JSPS).

[1] S. Takamura *et al.*, Plasma Fusion Res. **1**, 051 (2006).
[2] M. de Respinis *et al.*, ACS Appl. Mater. Interface **5**, 7621 (2013).
[3] S. I. Krasheninnikov, Phys. Scr. **T145**, 014040 (2011).
[4] Yu.V. Martynenko and M.Yu. Nagel, Plasma Phys. Rep. **38**, 12, 996 (2012).
[5] S. Kajita *et al.*, New J. Phys. **17**, 043038 (2015).
[6] K.B. Woller, D.G. Whyte and G.M. Wright, Nucl. Fusion **57**, 066005 (2017).
[7] S. Kajita *et al.*, Sci. Rep. (to be published in).
[8] R.D. Smirnov and S.I. Krasheninnikov, Nucl. Fusion **53**, 082002 (2013).
[9] S. Kajita *et al.*, Sci. Rep. **6**, 30380 (2016).
[10] S. Takamura and T. Uesugi, Appl. Surf. Sci. **356**, 888 (2015).
[11] S. Kajita *et al.*, Nucl. Fusion **49**, 095005 (2009).
[12] J.K. Tripathi *et al.*, Appl. Surf. Sci. **353**, 1070 (2015).
[13] J. Merker *et al.*, Platinum Metals Rev. **45**, (2), 74 (2001).
[14] E.P. Papadakis *et al.*, J Appl. Phys. **45**, 6 (1974).
[15] N. Ohno *et al.*, Nucl. Fusion **41**, 8 (2001).
[16] S. Kajita *et al.*, J. Nucl. Mater. **418**, 152 (2011).
[17] S. Kajita *et al.*, Surf. Coats. Tech. **340**, 86 (2018).
[18] K. Wang *et al.*, Sci. Rep. **7**, 42315 (2017).
[19] M. Yajima *et al.*, J. Nucl. Mater. **449**, 9 (2014).
[20] A. Litnovsky *et al.*, Fusion Eng. Des. **123**, 674 (2017).
[21] T.B. Massalski *et al.*, *Binary Alloy Phase Diagrams* **5** (ASM international 1990).